WPJET4 Gamma Spectrometer Upgrade (GSU)

D04	Design of a gamma-ray Detector Module 2 included: scintillator, photomultiplier, magnetic shielding, voltage divider and (preliminary) high voltage power supply. *31 December 2014*

On JET the α-particle diagnostic is based on the nuclear reaction $^{9}Be(\alpha,n\gamma)^{12}C$ between confined α-particles and beryllium impurity ions typically present in the plasma, *see GSU Project Management Plan* and references therein. The applicability of gamma-ray diagnostic is strongly dependent on the fulfilment of rather strict requirements for the definition and characterization of the neutron and gamma radiation fields (detector Field-of-View, radiation shielding and attenuation, parasitic gamma-ray sources). For operating this diagnostic at the high DT neutron fluxes expected in the future high-power DT campaign on JET, specific improvements are needed in order to provide good quality measurements in the D-T campaign, characterized by a more challenging radiation environment.

In order to enable the gamma-ray spectroscopy diagnostic for α-particle diagnostic during the DT campaigns the following goals should be achieved:

- Maximization of the signal-to-background ratio at the spectrometer detector; this ratio is defined by terms of the plasma-emitted gamma radiation and the gamma-ray background.
- Establishing high count rate signal processing and energy-resolved gamma-ray detection.

In the DT experiments the gamma-ray detector must fulfil requirements for high count rate measurements. The existent BGO-detector with a relatively long decay time, about 300 ns, should be replaced by a new detector module (DM2) based on $CeBr_3$ scintillator, with an associated digital data acquisition system. The $CeBr_3$ scintillator are characterized by short decay time (~20 ns) and a high light yield about 45 000 photons/MeV. The coupling of the scintillators with photomultiplier tubes in specially designed detector modules will permit the operation at count rates over 2 Mcps. The $CeBr_3$ scintillator is an alternative to the already tested at JET detectors based on $LaBr_3$.
The $CeBr_3$ scintillator was found to fulfil low noise measurement conditions. It shows 30 times reduction in internal activity in comparison with $LaBr_3$. The $CeBr_3$ scintillator has a similar energy resolution, sensitivity and decay time as the $LaBr_3$ scintillator. Moreover, the $CeBr_3$ scintillator seems to be more resistant for gamma radiation than $LaBr_3$. A 1 kGy dose of gamma radiation deteriorates the yield of $LaBr_3$ by ~10% and worsens its energy resolution from 3.0 to 3.8%, while is almost negligible for $CeBr_3$.
$CeBr_3$ may also be more resistant to neutron radiation because of lower neutron capture cross section in Ce (~12 mb) than in La (~100 mb) at E_n ~30 keV [1-2].
These features make $CeBr_3$ an interesting alternative for JET plasma applications in spite of the excellent spectroscopic performances of $LaBr_3$ scintillator.

At NCBJ we used, an available from another our project, a detector system based on 3"×3" $CeBr_3$ coupled to a Hamamatsu R6233 photomultiplier (from SCIONIX) and performed measurements on energy resolution and detection efficiency. For measurements we used:

- standard radioactive sources (see Table 1),
- a PuBe source emitting gamma-rays with an energy of 4.4 MeV,
- a PuC source emitting gamma-rays with an energy of 6.1 MeV.

We also measured background in our laboratory for each detector set-up.

1. Measurements at NCBJ with 3"×3" $CeBr_3$ and Hamamatsu R6233 (from SCIONIX)

All measurements were done at our laboratory at NCBJ. Signal from the PMT was sent to CANBERRA preamplifier and then, to ORTEC spectroscopy amplifier. Finally, the Gaussian shaped signal was registered by TUKAN 8K USB multichannel analyser. The distance between radioactive sources and scintillator surface was set to 54 cm.

Fig. 1 shows measured gamma spectra for the 3"×3" $CeBr_3$ scintillator. Left part of this figure presents spectra registered for ^{137}Cs and ^{22}Na sources. In both cases we registered also 1460 keV full energy peak originating from natural background (^{40}K isotope). In the right part of Fig.1, high energy parts of spectra measured for the PuBe and PuC sources are shown. We can distinguish full energy peak (FEP), single escape peak (SEP), which is 0.511 MeV lower and double escape peak (DEP) lower by 1.022 MeV. In this energy range, we didn't observe any peak structure in background.

For comparison, similar measurements were done with a 3"×3" $LaBr_3$ scintillator. Obtained spectra are presented in Fig. 2. Low energy part of spectrum in $LaBr_3$ has more complicated structure due to scintillator self-activity from La isotopes, see above. These effects are very well visible in background measurements, especially for gamma-ray energies about 1 MeV.

We also compared measured energy resolution (Fig. 3) and full energy peak (FEP) detection efficiency (Fig. 4) for both scintillators. In Tables 1 and 2, values for selected calibration sources are shown. The energy resolution is defined as a ratio of full width at half maximum divided by the energy of the recorded peak.
For $CeBr_3$, as well as for the $LaBr_3$ scintillator, we observed a deterioration of the energy resolution for 4.4 MeV gamma rays from the PuBe source. The peak broadening was also noticed for single and double escape peak from this source. We assign this effect to Doppler broadening [3] and we plan to study this problem in future. This effect is not present for 6.1 MeV gamma rays from the PuC source.

Full energy peak detection efficiency ε was calculated using the following equation:

$$\varepsilon = \frac{N}{A \times b \times t \times \omega}$$

where:

N – number of counts in full energy peak (background subtracted),
A – source activity,
t – live time of the measurement,
ω – solid angle of detection,
b – branching ratio of the reaction resulting in gamma-ray emission.

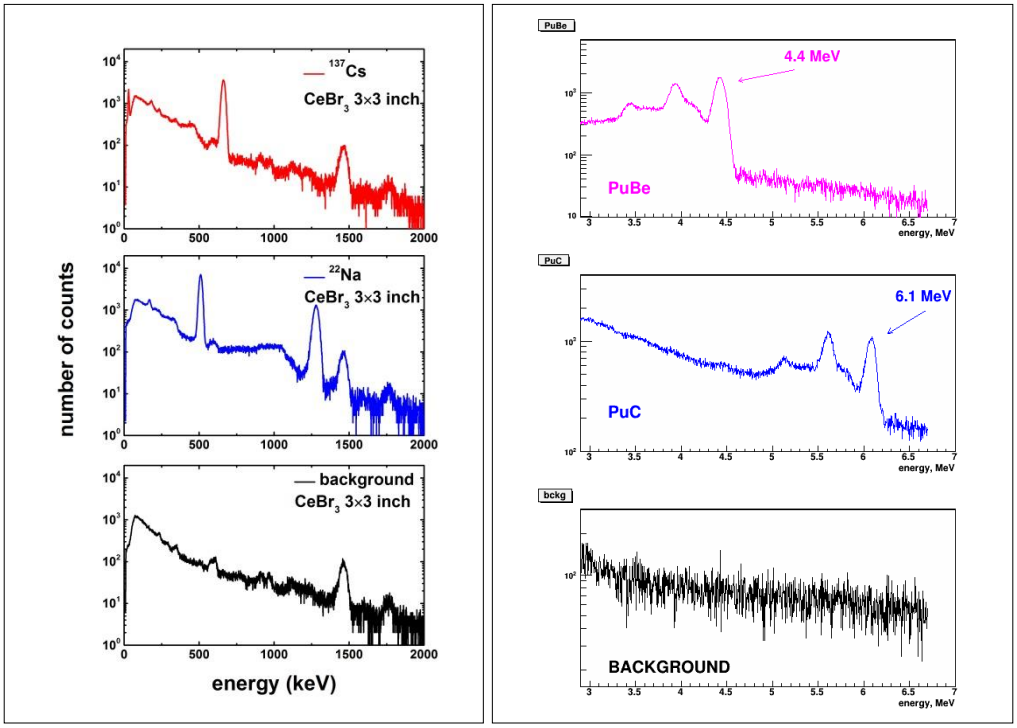

Fig. 1. Gamma-ray spectra measured with 3"×3" $CeBr_3$ scintillator. *Left*: spectra recorded for ^{137}Cs and ^{22}Na. The 1.46 MeV line is connected with a natural ^{40}K isotope. *Right*: measurements with the PuBe and PuC sources. The full energy (marked by values), single escape and double escape peaks are seen. In the lower part, the measured background is shown.

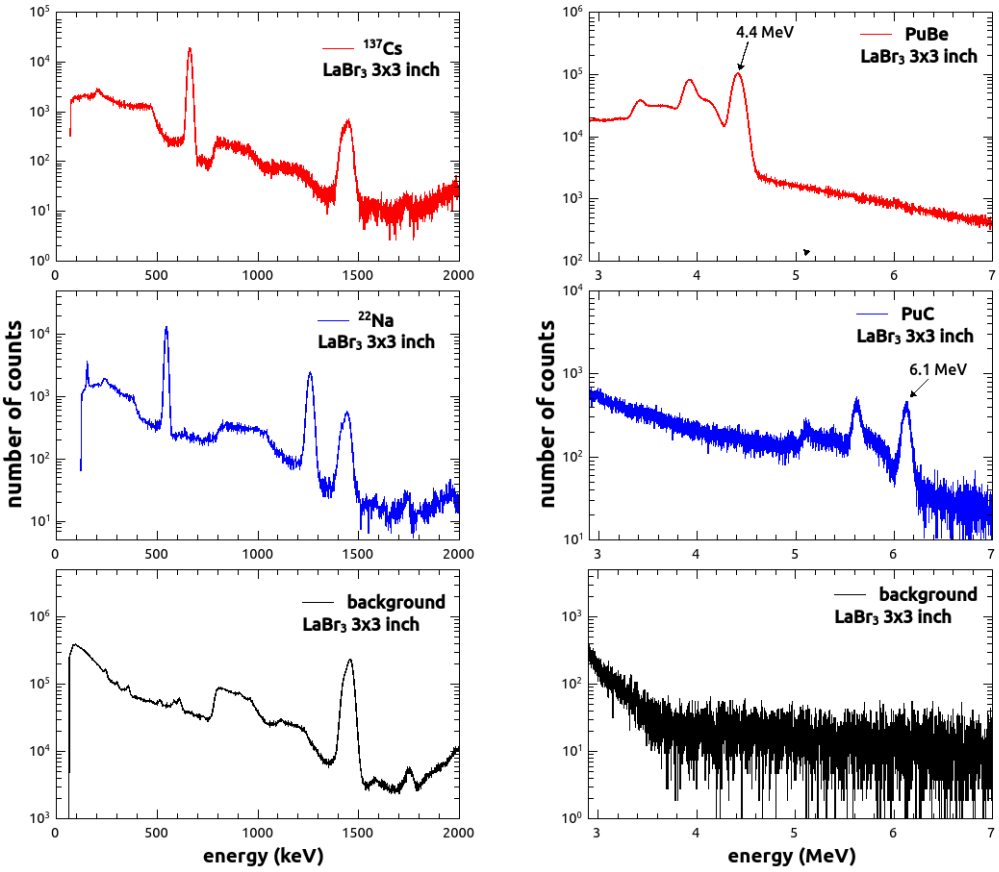

Fig. 2. Gamma-ray spectra measured with 3"×3" $LaBr_3$ scintillator. *Left*: spectra for ^{137}Cs and ^{22}Na sources. The 1.46 MeV line is connected with a natural 40K isotope. *Right*: measurements with the PuBe and PuC sources. The full energy (marked by values), single escape and double escape peaks are seen. In the lower part, the measured background is shown.

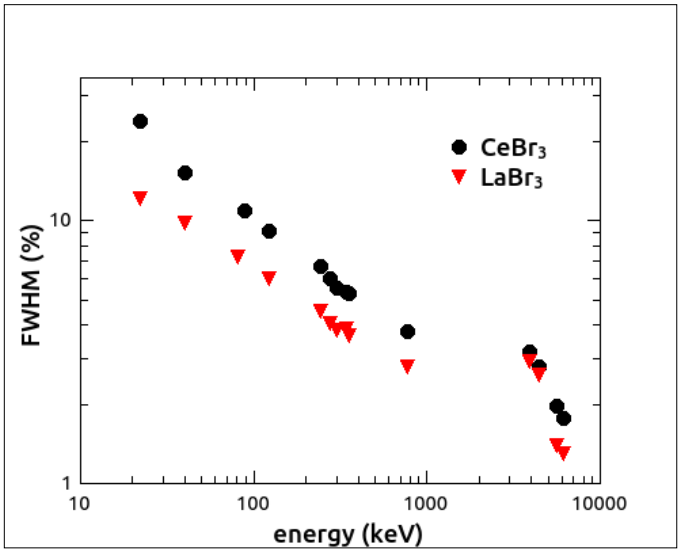

Fig. 3. Comparison of energy resolution obtained for 3"×3" $CeBr_3$ (black circle) and 3"×3" $LaBr_3$ (red triangle) scintillators with standard radioactive sources, as well as with the PuBe and the PuC sources, see Table 1.

Table 1. Energy resolution measured for 3"×3" $CeBr_3$ and $LaBr_3$ scintillators for selected radioactive sources. Errors in average are estimated to be about ±0.2 %.

Source	Energy (keV)	FWHM (%)	
		$CeBr_3$	$LaBr_3$
^{22}Na	511.0	4.5	3.4
^{137}Cs	661.7	4.0	3.0
^{22}Na	1274.5	3.1	2.4
PuBe (SEP)	3927*	3.3	2.9
PuBe (FEP)	4438*	2.8	2.6
PuC (SEP)	5618	2.0	1.4
PuC (FEP)	6129	1.8	1.3

(*) Deterioration of energy resolution due to the Doppler broadening [3].

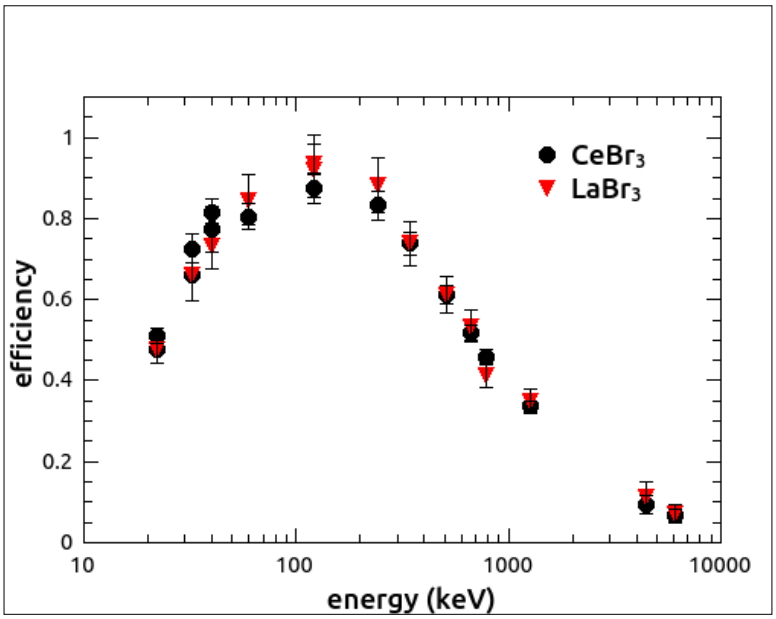

Fig. 4. Comparison of FEP detection efficiency obtained for 3"×3" $CeBr_3$ (black circle) and 3"×3" $LaBr_3$ (red triangle) scintillators with standard radioactive sources as well as with PuBe and PuC sources. See also Table 2.

Table 2. Full energy peak detection efficiency determined for 3"×3" $CeBr_3$ and $LaBr_3$ scintillators for selected radioactive sources and X- or gamma-ray lines given in column 2.

Source	Energy (keV)	Efficiency	
		$CeBr_3$	$LaBr_3$
Ag (K_α)	22.1	0.512 ± 0.019	0.477 ± 0.035
Ba (K_α)	32.1	0.725 ± 0.036	0.659 ± 0.062
Sm (K_α)	39.9	0.815 ± 0.033	0.773 ± 0.056
^{241}Am	59.5	0.804 ± 0.032	0.846 ± 0.062
^{22}Na	511.0	0.612 ± 0.023	0.611 ± 0.045
^{137}Cs	661.7	0.518 ± 0.020	0.534 ± 0.039
^{22}Na	1274.5	0.337 ± 0.013	0.349 ± 0.029
PuBe	4438	0.094 ± 0.024	0.112 ± 0.040
PuC	6129	0.066 ± 0.016	0.073 ± 0.019

Conclusions from measurements

1. in case of $CeBr_3$, for energies about 1 MeV no internal activity in comparison with $LaBr_3$ is observed, see Fig. 1 and 2, left lower parts. For energies about few MeV, spectrum measured for $LaBr_3$ does not show any structure as in case of $CeBr_3$, right lower parts,
2. in average, lower energy resolution by ~10% for $CeBr_3$ in comparison with $LaBr_3$, see Table 1,
3. similar FEP detection efficiency for both $CeBr_3$ and $LaBr_3$ scintillators, see Table 2.

2. Schematic design of $CeBr_3$ with a connector for optical fiber

1. According to the results presented in the previous section, see Conclusions from measurements, a scintillation detector based on 3" diameter and 3" height $CeBr_3$ crystal with a photomultiplier readout is well suited for gamma-ray spectrometry of high energy gamma-rays produced during plasma experiments at JET.
2. The detector will be connected to a voltage divider designed for high counting rates. The PMT will be supplied with negative high voltage through an SHV connector. The signals from the anode output will be sent to a BNC connector, allowing for direct registration of the signals by the digital acquisition electronics.
3. The detector proposed for the GSU project includes an FC connector that allows to inject light via an optical fiber at the backside of the PMT. This solution will be used in order to control the possible PMT gain drifts and, eventually, apply corrections for spectra energy calibration.

4. All connectors will be placed at the rear side of the detector.
5. The detector will be partially covered with a 1 mm thick μ-metal shielding in order to reduce possible influence of the magnetic field on the performance of the detector.
6. The length of the encapsulated detector amounts to 240 mm (excluding connectors) and the diameter equals to 83.9 mm, according to the schematic drawing presented in Fig. 5. We estimate that connector length is less than 3 cm. The final dimensions will be decided on the base of an updated schematic drawing from SCIONIX.
7. The detector will be installed inside the KM6T gamma-ray detector tunnel by means of a dedicated detector carrier. It is decided to use one detector module at a time [4].
8. The estimated price for a complete detector with a connector for optical fiber is about 35 kEuro +23%VAT, added to ~44 kEuro, and a delivering time is about 3 months.

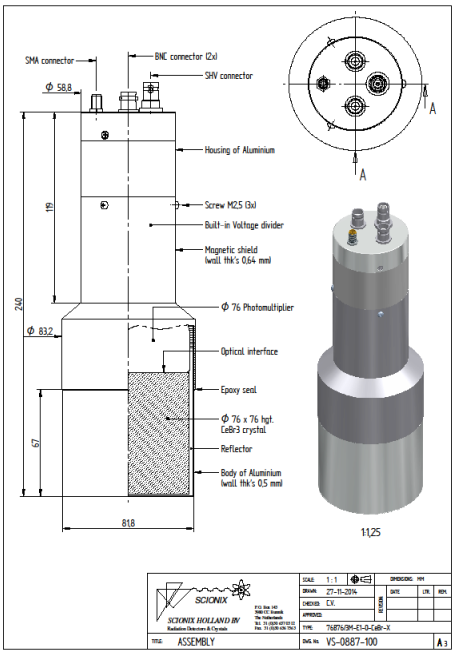

Fig. 5. The schematic design of the detector for GSU as sent by SCIONIX.

References

[1] H. Beer et al., „Neutron capture cross section on ^{138} Ba, ^{140,142}Ce, ^{175,176}Lu and ^{181}Ta at 30 keV", Phys. Rev. C **21** (1980) 534.

[2] A. Musgrove, „Resonant neutron capture in ^{139}La", Australian Journal of Physics **30** (1977) 599.

[3] Glenn F. Knoll, „Radiation Detection and Measurement”, 3rd edition (2010).
[4] Minutes of the GSU Project Meeting on 2014/11/18.